Article

Identification and Correlation Analysis of Ferroptosis-Related Genes in Three Brain Regions of Patients with Schizophrenia

Shiqin Dai[1]
Yong Xu[2]
Tingting Yang[3]
Feng Wang[1]
Yihua Jiang[1,*]

[1]Prevention and Treatment Department, Shanghai Minhang District Mental Health Center, 201112 Shanghai, China
[2]School of Life Sciences, East China Normal University, 200241 Shanghai, China
[3]General Office, Shanghai Clinical Laboratory Center, 200126 Shanghai, China

Abstract

Background: Schizophrenia (SZ) is a severe mental disorder that is marked by hallucinations and cognitive impairments. Ferroptosis is a type of cell death that is associated with iron and lipid peroxidation; it may play a role in SZ etiology. The present study aimed to explore the correlations between ferroptosis-related genes and SZ in three brain regions.

Methods: We used the Gene Expression Omnibus dataset GSE80655 to analyze brain samples from SZ patients and controls; specifically, we evaluated the anterior cingulate cortex (Ancg), dorsolateral prefrontal cortex (DLPFC), and nucleus accumbens (nAcc). The data were preprocessed in R, and ferroptosis-related differentially expressed genes (DEGs) were identified. Pearson correlation analysis was then performed to assess correlations between these DEGs and age at death, postmortem interval, or brain pH. To identify important ferroptosis-related genes, we created a protein–protein interaction network using the Search Tool for the Retrieval of Interacting Genes/Proteins database, and visualized it using Cytoscape software. Moreover, the pROC package was used to calculate the area under the receiver operating characteristic curves for these important genes. Finally, gene set variation analysis was used for the pathway enrichment analysis of ferroptosis-related pathways, followed by the Wilcoxon rank-sum test.

Results: Nine ferroptosis-related DEGs were upregulated in the Ancg region and one was downregulated in the nAcc region. In the Ancg region, the SZ group had four ferroptosis-related DEGs that were negatively correlated with postmortem interval, and the control group had five ferroptosis-related DEGs that were negatively correlated with brain pH. The protein–protein interaction network analysis of the Ancg region revealed seven significant interacting genes; tissue inhibitor of metalloproteinases 1 (*TIMP1*) and galectin 3 (*LGALS3*) were the hub genes. Gene set variation analysis revealed substantial changes in the glycolysis pathway in the Ancg region, and in the glutamate transmembrane transport pathway and unsaturated fatty acid biosynthesis process pathway in the nAcc region, in SZ patients compared with controls.

Conclusions: The correlation between ferroptosis and SZ appears to be stronger in the Ancg than in the nAcc or dorsolateral prefrontal cortex. This association may be mediated by *TIMP1* and *LGALS3* as well as by the glycolysis pathway, indicating that these might be possible biomarkers for SZ.

Keywords

ferroptosis-related genes; schizophrenia; three brain regions; ferroptosis-related pathways; postmortem interval; brain pH

Introduction

Positive symptoms of schizophrenia (SZ) include hallucinations and delusions, whereas negative symptoms include emotional apathy, social disengagement, and cognitive failure. SZ frequently manifests as recurring episodes that are difficult to treat or reduce [1]. It is a complex, se-

*Corresponding author details: Yihua Jiang, Prevention and Treatment Department, Shanghai Minhang District Mental Health Center, 201112 Shanghai, China. E-mail: janelzs@sohu.com

vere mental illness with a poorly understood cause [2,3]. Related studies suggest that SZ is a psychiatric illness caused by a combination of environmental and genetic variables [4–7]. Notably, perinatal period iron insufficiency may be a risk factor for SZ development; animal trials, human investigations, and epidemiological surveys all provide evidence to support this viewpoint [8]. Furthermore, a meta-analysis of data from 39 investigations of plasma and serum revealed the common incidence of iron deficiency in patients with SZ [9]. Magnetic resonance neuroimaging studies of patients with SZ have demonstrated significantly elevated brain iron levels in areas such as the striatum and thalamus [10,11]. Iron is essential for the central nervous system, where it participates in neurophysiological functions such as neurotransmitter production, redox balance, and myelination [12]. Thus, abnormalities in brain iron metabolism may play an important role in the onset and progression of SZ [3]. Ferroptosis is a type of programmed cell death that is mostly mediated by cellular metabolic pathways. These pathways include redox homeostasis, iron metabolism, mitochondrial function, and amino acid, lipid, and glucose metabolism, all of which are affected by disease-associated signaling pathways [13].

As a relatively new research field, the number of published papers on ferroptosis has experienced exponential growth in recent years [13]. Ferroptosis is reportedly important in neurological disorders [14]; however, research into ferroptosis in SZ is relatively limited. To date, the relationship between ferroptosis-related genes and SZ has been explored in only one study, which used samples from peripheral blood mononuclear cells and the prefrontal brain [15].

The anterior cingulate cortex (Ancg), dorsolateral prefrontal cortex (DLPFC), and nucleus accumbens (nAcc) are commonly associated with emotional changes, cognition, impulse control, motivation, reward, and pleasure—all of which are altered in mental disorders [16]. In the present study, we therefore selected these three brain regions to investigate ferroptosis-related genes in SZ, to fill the research gap in this area. Transcriptome data from SZ patients and a control group in the GSE80655 dataset of the Gene Expression Omnibus (GEO) were used to investigate the ferroptosis-related genes and pathways in these three brain regions. We also explored the associations between ferroptosis-related differentially expressed genes (DEGs) and age at death, postmortem interval, or brain pH. This study not only aids in our understanding of the pathophysiology of SZ, but also offers novel insights and potential clinical intervention strategies for this disease.

Materials and Methods

Dataset Selection and Analysis

The GEO is a publicly accessible gene expression database that is operated by the National Center for Biotechnology Information (USA). It is primarily used to store and publicly share gene expression data as well as other types of high-throughput sequencing data [17]. The GSE80655 dataset was downloaded from the GEO database (https://www.ncbi.nlm.nih.gov/geo/) based on the disease type of the study. This dataset contains 141 samples: 71 from SZ patients (24 Ancg, 24 DLPFC, and 23 nAcc) and 70 from controls (24 Ancg, 24 DLPFC, and 22 nAcc). The original studies from which these data were derived followed ethical guidelines in accordance with the Declaration of Helsinki. We processed the dataset using R (version 4.4.0, R Foundation for Statistical Computing, Vienna, Austria) with AnnotationDbi, parallel, BiocGenerics, Biobase, IRanges, S4Vectors, and openxlsx packages. We used the mapIds function from the org.Hs.eg.db package (version 3.19.1, Bioconductor, Seattle, WA, USA) to translate ENSEMBL IDs to gene names. We then cleaned the data, deleting any probable missing values. Finally, gene expression information from the three brain regions was collected.

Identification of DEGs

To compare whether genes were differentially expressed between the SZ and control groups, we used the edgeR package (version 4.2.0, Walter and Eliza Hall Institute of Medical Research, Melbourne, Victoria, Australia) [18] to analyze the GSE80655 dataset for DEGs. Significant DEGs were filtered based on a fold-change threshold of >1.5 and a false discovery rate (FDR) threshold of <0.05. Genes with log2FC >0 were taken as upregulated, whereas genes with log2FC <0 were taken as downregulated. To create volcano plots, the geom_point function from the ggplot2 library was used.

Extraction of Ferroptosis-Related DEGs

The ferroptosis-related genes were primarily obtained through a literature review [19]. The intersection between the DEGs obtained in the previous step and these ferroptosis-related genes yielded ferroptosis-related DEGs. To do this, we drew Venn diagrams using the grid (version 4.4.0, R Foundation for Statistical Computing, Vienna, Austria) and VennDiagram (version 1.7.3, Ontario Institute for Cancer Research, Toronto, ON, Canada) pack-

Yihua Jiang, *et al.*

Identification and Correlation Analysis of Ferroptosis-Related Genes in Three Brain Regions of Patients with Schizophrenia

ages; any overlaps between our identified DEGs and the 855 ferroptosis-related genes represent ferroptosis-related DEGs.

Correlation Analysis between Ferroptosis-Related DEGs and Parameters such as Age of Death, Postmortem Interval, or Brain pH

Using the ferroptosis-related DEGs between the SZ and control groups, we used R to conduct a Pearson correlation analysis between the DEGs and age at death, postmortem interval, or brain pH. We then created a correlation bubble plot using the ggplot2 (version 3.5.1, Austin, TX, USA) and ggrepel (version 0.9.5, Boston, MA, USA) packages.

Creation of the Protein–Protein Interaction (PPI) Network and Selection of Hub Genes

We uploaded the names of our identified ferroptosis-related DEGs to the Search Tool for the Retrieval of Interacting Genes/Proteins (STRING) database (version 12.0, European Molecular Biology Laboratory, Heidelberg, Germany; https://string-db.org/) [20] to construct a PPI network. We then imported the results from the STRING database analysis into Cytoscape software (version 3.10.2, Institute for Systems Biology, Seattle, WA, USA) [21] and used the built-in cytoHubba plugin [22] to perform subnetwork selection and visualization. The Degree algorithm was used for topology analysis and gene relevance ranking in critical subnetworks, resulting in the identification of hub ferroptosis-related genes.

Evaluation of the Diagnostic Value of Ferroptosis-Related Hub Genes

To further explore the diagnostic value of hub genes in SZ, the pROC package (version 1.18.5, Geneva, Switzerland) [23] was used to plot the receiver operating characteristic [24] curves in the Ancg region based on the hub genes tissue inhibitor of metalloproteinases 1 (*TIMP1*) and galectin 3 (*LGALS3*), and in the nAcc region based on activating transcription factor 3 (*ATF3*). A greater area under the curve (AUC) [25] suggests more potential utility for these genes in the diagnosis of SZ.

Analysis of Gene Set Variation in Ferroptosis-Related Pathways

The gene list associated with ferroptosis pathways was mostly gathered from relevant literature [19]. The gene set

variation analysis (GSVA; version 1.52.3, Barcelona, Catalonia, Spain) [26] program was used to perform enrichment analysis of the ferroptosis-related pathways, which resulted in GSVA enrichment scores for the three brain regions. The Wilcoxon rank-sum test was then used to compare the GSVA scores of ferroptosis-related pathways between the SZ and control groups in each of the three brain regions. $p < 0.05$ indicates significance. To create violin plots, we used the ggplot2, Hmisc (version 5.1.3, Nashville, TN, USA), and ggalluvial (version 0.12.5, Farmington, CT, USA) [27] packages in R.

Results

Identification of DEGs

Significant DEGs between the SZ and control groups were observed in all three brain regions. In the Ancg, DLPFC, and nAcc regions, there were significant changes in gene expression levels; specifically, there were 253 DEGs (233 upregulated, 20 downregulated) in the Ancg (Fig. 1A), five DEGs (three upregulated, two downregulated) in the DLPFC (Fig. 1B), and 167 DEGs (157 upregulated, 10 downregulated) in the nAcc (Fig. 1C).

Extraction of Ferroptosis-Related DEGs

In the Ancg region, nine ferroptosis-related DEGs were identified (FDR <0.05): interferon-induced transmembrane protein 3 (*IFITM3*), hypoxia inducible factor 3 subunit alpha (*HIF3A*), *TIMP1*, lipin 3 (*LPIN3*), NAD(P)H quinone dehydrogenase 1 (*NQO1*), phospholipase A1 member A (*PLA1A*), *LGALS3*, ceruloplasmin (*CP*), and caspase 4 (*CASP4*), all of which were upregulated (Fig. 2A,B). The significant expression changes of these genes suggest the potential importance of the Ancg for iron metabolism regulation. By contrast, no significant ferroptosis-related DEGs were identified in the DLPFC. In the nAcc, only one ferroptosis-related DEG was identified: *ATF3*, which was downregulated (Fig. 2C,D). These results not only demonstrate that differential expression patterns of iron metabolism regulation occur across different brain regions, but also suggest the potential existence of region-specific biological functions.

Correlation Analysis between Ferroptosis-Related DEGs and Factors such as Age at Death, Postmortem Interval, or Brain pH

In the Ancg, we observed significant correlations between ferroptosis-related DEGs and postmortem interval
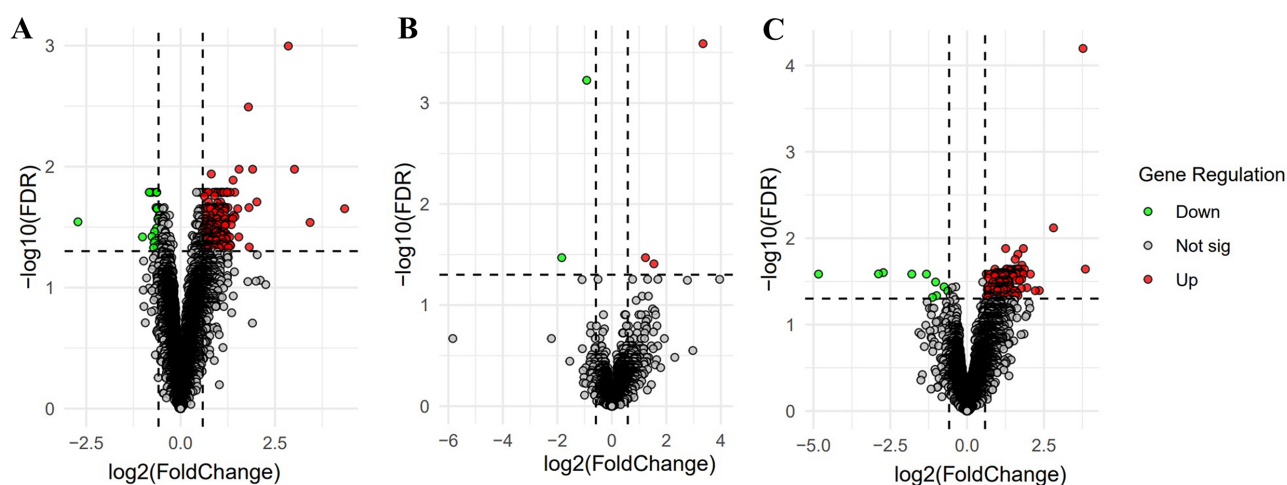
Fig. 1. Volcano plots of differentially expressed genes (DEGs) between the schizophrenia and control groups across three brain regions. (A) Anterior cingulate cortex. (B) Dorsolateral prefrontal cortex. (C) Nucleus accumbens. Red dots represent significantly upregulated genes, green dots represent significantly downregulated genes, and gray dots represent non-significant DEGs.

as well as brain pH values in the SZ and control groups. Specifically, four ferroptosis-related DEGs in the SZ group were negatively correlated with postmortem interval: *CP* ($r = -0.41$, $p = 0.044$), *LGALS3* ($r = -0.41$, $p = 0.045$), *LPIN3* ($r = -0.55$, $p = 0.006$), and *HIF3A* ($r = -0.42$, $p = 0.043$) (Fig. 3A). In the SZ group, ferroptosis-related genes were primarily influenced by postmortem interval, suggesting that these genes may be regulated by specific pathological factors, such as iron homeostasis imbalance and oxidative stress, that were present during the disease state. These pathological factors may have already existed in these patients before their death and continued to affect gene expression postmortem. Furthermore, in the control group, five ferroptosis-related DEGs were negatively correlated with brain pH: *PLA1A* ($r = -0.48$, $p = 0.017$), *CP* ($r = -0.46$, $p = 0.022$), *TIMP1* ($r = -0.50$, $p = 0.012$), *IFITM3* ($r = -0.43$, $p = 0.037$), and *LGALS3* ($r = -0.48$, $p = 0.017$) (Fig. 3B). In the control group, these genes may have maintained normal brain function and metabolic homeostasis by responding to fluctuations in brain pH. These correlations likely reflect the adaptive mechanism of the normal brain to pH fluctuations. The differential expression of common genes between the two groups, such as *CP* and *LGALS3*, further highlights the disease-specific regulatory mechanisms. In the SZ group, the expression of these genes was more susceptible to pathological factors (such as a prolonged postmortem interval, leading to sustained oxidative stress and inflammatory responses), whereas in the control group, these genes responded more to normal physiological changes (such as pH fluctuations). By contrast, no correlations were identified in the nAcc region.

Creation of the PPI Network and Selection of Hub Genes

We uploaded the nine ferroptosis-related DEGs to the STRING database and removed two isolated nodes without connections, resulting in a PPI network structure that was composed of seven nodes and fourteen edges (Fig. 4A). The results of the PPI network analysis were imported into Cytoscape, and two hub genes—*TIMP1* and *LGALS3*—were identified using the Cytohubba plugin. This finding indicates that these two genes are the most important nodes of the network, and may play crucial roles in the mechanism of iron homeostasis (Fig. 4B).

Evaluation of the Diagnostic Value of Ferroptosis-Related Hub Genes

In the Ancg region, we investigated the diagnostic value of *TIMP1* and *LGALS3*. They had AUC values of 0.63 and 0.64, respectively (Fig. 5A), indicating that *TIMP1* and *LGALS3* may have the potential to distinguish patients with SZ. In the nAcc region, we observed an AUC value of 0.61 for *ATF3* (Fig. 5B), further highlighting its potential role as a biomarker in SZ. The combined examination of *TIMP1* and *LGALS3* in the Ancg region revealed their potential diagnostic value for SZ, with a combined AUC value of 0.65 (Fig. 5C). These results provide a basis for further research into the role of *TIMP1* and *LGALS3* in SZ.
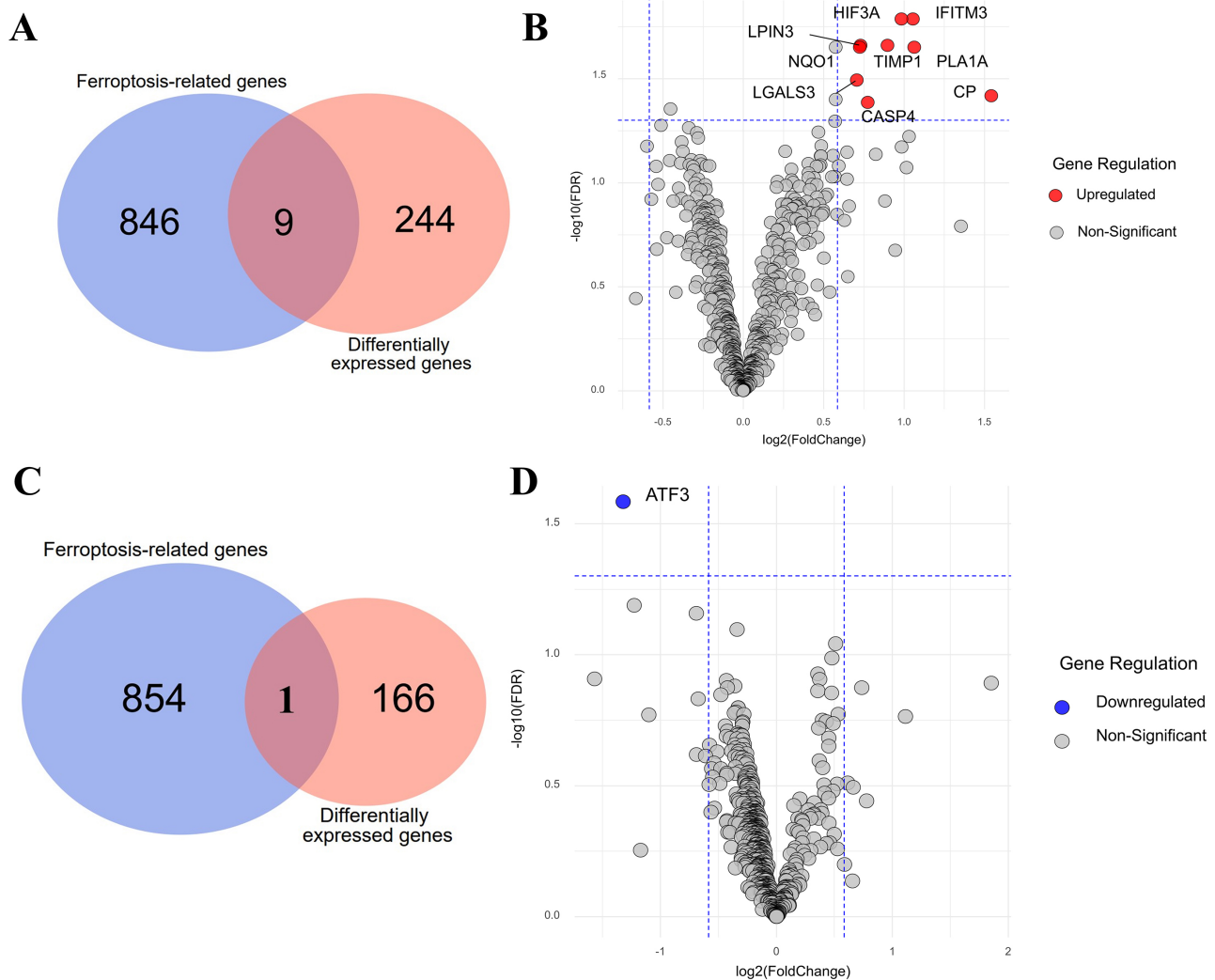
Fig. 2. Venn plots of differentially expressed genes (DEGs) and ferroptosis-related genes in the anterior cingulate cortex (Ancg) and nucleus accumbens (nAcc), and correlation volcano plots of ferroptosis-related DEGs in these brain regions. (A,B) Ancg. (C,D) nAcc. (A,C) The blue portion represents ferroptosis-related genes, the red portion represents DEGs, and the overlapping portion represents ferroptosis-related DEGs. (B,D) Red dots represent significantly upregulated genes, blue dots represent significantly downregulated genes, and gray dots represent non-significant DEGs. *LPIN3*, lipin 3; *HIF3A*, hypoxia inducible factor 3 subunit alpha; *IFITM3*, interferon-induced transmembrane protein 3; *NQO1*, NAD(P)H quinone dehydrogenase 1; *LGALS3*, galectin 3; *TIMP1*, tissue inhibitor of metalloproteinases 1; *PLA1A*, phospholipase A1 member A; *CP*, ceruloplasmin; *CASP4*, caspase 4.

Analysis of Gene Set Variation in Ferroptosis-Related Pathways

Relative to the control group, the SZ group had significant changes ($p < 0.05$) in the Ancg region for one ferroptosis-related pathway: the glycolysis pathway (Fig. 6A). The glycolysis pathway breaks down glucose to generate Adenosine Triphosphate/energy and provides the raw materials required for cellular biosynthesis. Compared with the control group, the SZ group had abnormal downregulation of the glycolysis pathway; this may affect cellu-

lar energy metabolism, biosynthesis, and neuronal function and survival. Ferroptosis-related metabolic abnormalities may play an important role in this process. There were no substantial variations in ferroptosis-related pathways in the DLPFC region. In the nAcc region, two ferroptosis-related pathways exhibited substantial changes ($p < 0.05$) in the SZ group: those of glutamate transmembrane transport and unsaturated fatty acid biosynthesis (Fig. 6B,C). The glutamate transmembrane transport pathway regulates the distribution and concentration of glutamate in the nervous system, thus critically influencing neurotransmission and neuronal ex-
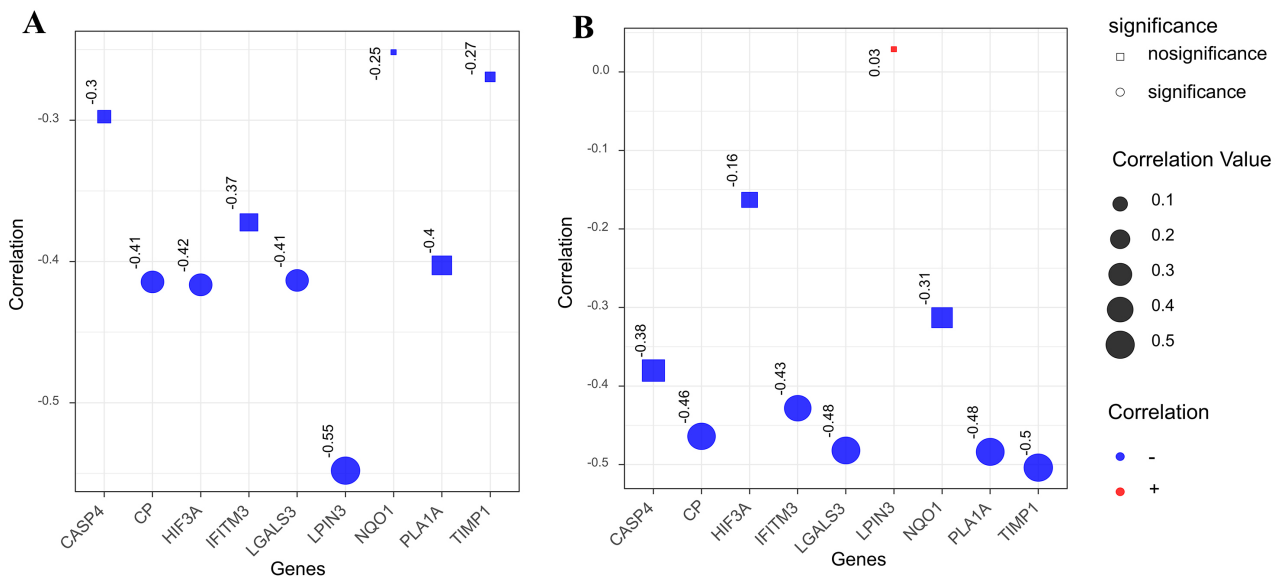
Fig. 3. Bubble plots of correlations between ferroptosis-related differentially expressed genes (DEGs) and postmortem interval or brain pH in the anterior cingulate cortex region. (A) In the schizophrenia group, four ferroptosis-related DEGs were negatively correlated with postmortem interval. (B) In the control group, five ferroptosis-related DEGs were negatively correlated with brain pH. The size of the points represents the absolute value of the correlation coefficient, red indicates a positive correlation, blue indicates a negative correlation, and the shape of each point represents significance (circle for significance, square for no significance).
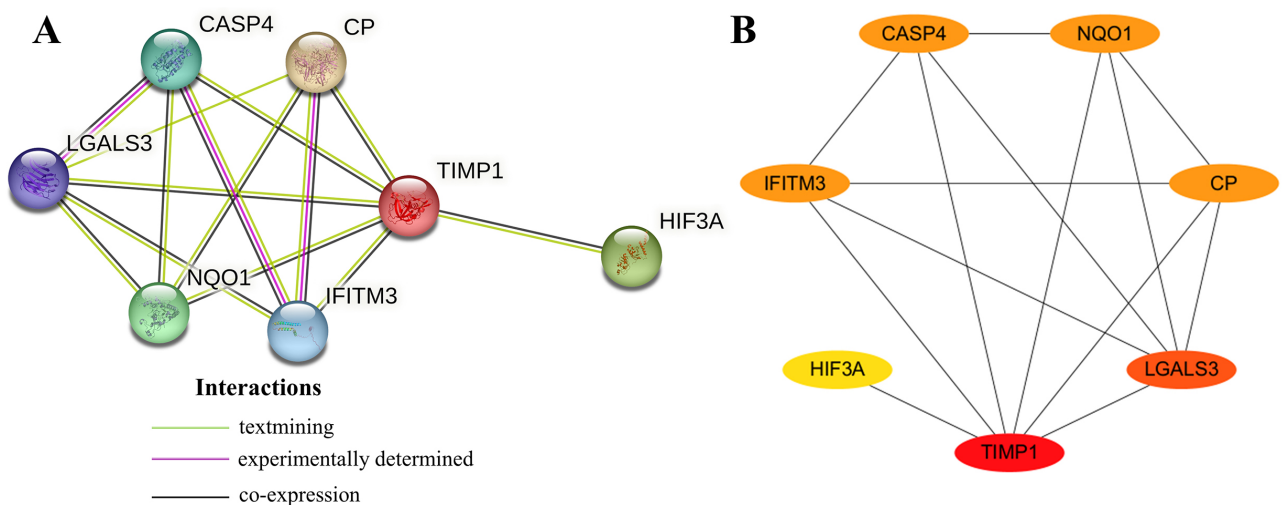
Fig. 4. Protein–protein interaction (PPI) network graph and hub gene network graph of ferroptosis-related differentially expressed genes (DEGs) in the anterior cingulate cortex (Ancg) region. (A) PPI network graph of ferroptosis-related DEGs in the Ancg. Purple lines represent experimentally determined interactions, green lines represent text mining interactions, and black lines represent co-expression interactions. (B) Hub gene network graph of the Ancg. A node color that approaches red indicates that the gene has higher centrality in the network.

citability and function. The unsaturated fatty acid biosynthesis pathway synthesizes the unsaturated fatty acids that are needed for cell membrane structure. This pathway is involved in regulating cellular energy storage, signal transduction, and bioactive molecule synthesis. Compared with the control group, the SZ group had downregulation of both the glutamate transmembrane transport pathway and the unsaturated fatty acid biosynthesis pathway. Because these are ferroptosis-related pathways, this finding may suggest that abnormal metabolic expression is associated with fer-
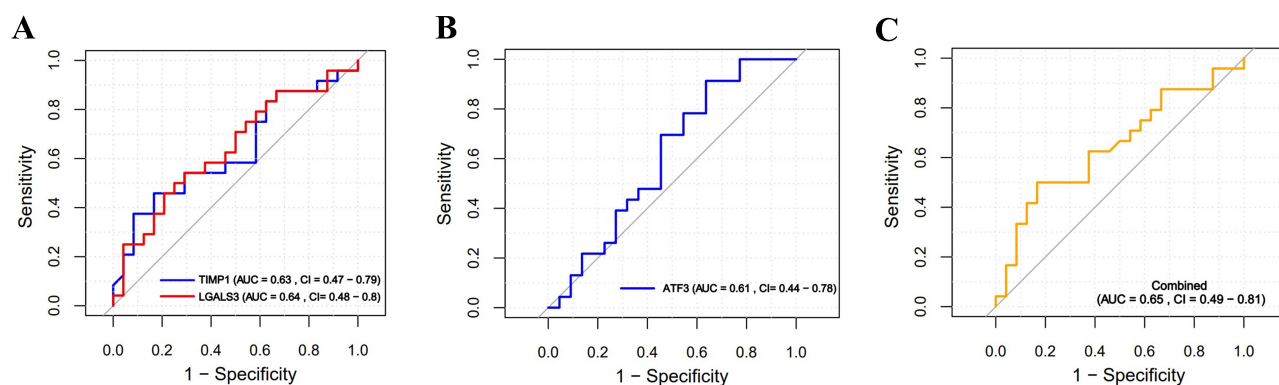
Fig. 5. Analysis of the diagnostic value of ferroptosis-related hub genes in the anterior cingulate cortex (Ancg) and nucleus accumbens (nAcc) regions. (A) Tissue inhibitor of metalloproteinases 1 (*TIMP1*) and galectin 3 (*LGALS3*) in the Ancg. (B) Activating transcription factor 3 (*ATF3*) in the nAcc. (C) The combined examination of hub genes *TIMP1* and *LGALS3* in the Ancg. The area under the curve (AUC) represents the receiver operating characteristic curve.

roptosis mechanisms in SZ patients. These changes may also be linked to neuronal dysfunction, alterations in cell membrane structure, and/or the development and progression of the disease.

Discussion

SZ is a complex neuropsychiatric condition that can be induced by a variety of circumstances. Previous research has revealed considerable genetic susceptibility and familial clustering in SZ, with pathophysiology strongly linked to genetics. Because of its possible importance in neurodegenerative diseases, ferroptosis—a unique form of controlled cell death—has recently received much interest [28–31]. However, the precise involvement of ferroptosis in SZ remains unknown. In the present work, we investigated ferroptosis-related DEGs in SZ and explored their probable causes using a gene expression analysis of three brain regions.

A large number of DEGs were identified in the Ancg, and the significant changes in these genes may reflect the crucial role of this brain region in the pathogenesis of SZ. By contrast, the DLPFC and nAcc exhibited fewer DEGs, suggesting that changes in gene expression in these areas might be more limited in SZ. The Ancg also had the highest number of ferroptosis-related DEGs. This finding implies that aberrant iron metabolism and the ferroptosis-related pathway may play major roles in the Ancg, and indicates that distinct brain regions may be involved in the development and progression of SZ via different molecular processes. In the nAcc, a significant downregulation of the ferroptosis-related DEG *ATF3* was observed. *ATF3* is a transcription factor that has important functions in cellu-

lar stress responses and neurological diseases [32–34]. Its downregulation in SZ patients may suggest the abnormal regulation of iron metabolism pathways and an involvement in complex mechanisms related to cell death and oxidative stress.

In the Ancg, the expression levels of some ferroptosis-related genes were negatively correlated with the postmortem interval. This suggests a possible association between metabolic abnormalities of these genes in the brains of SZ patients and clinical manifestations, further emphasizing the importance of iron metabolism abnormalities in the pathogenesis of SZ. However, no such correlation was observed in the other two brain regions.

Through PPI network analysis, *TIMP1* and *LGALS3* were identified as ferroptosis-related hub genes in the Ancg. These genes play crucial roles in extracellular matrix remodeling and cell death processes [35–37]. Moreover, the significant expression changes of these genes in SZ suggest their potentially important regulatory roles in the pathological processes of the disease, and indicate that they may serve as potential therapeutic targets.

Although *TIMP1*, *LGALS3*, and *ATF3* have demonstrated significant alterations in SZ research, their utility in the early detection of psychiatric disorders remains limited. This study investigates the role of these genes in pathological mechanisms and explores their potential value in multi-gene combination strategies. Future research should aim to enhance the accuracy of diagnostic models through the integration of multi-gene combinations and supplementary methods, and evaluate the clinical applicability of these genes.
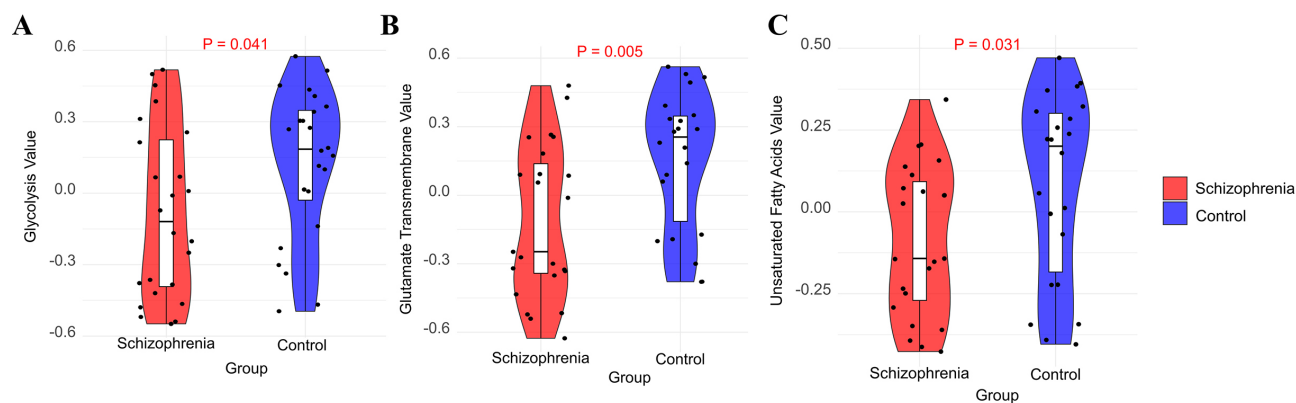
Fig. 6. Violin plots comparing the gene set variation analysis (GSVA) scores of ferroptosis-related pathways in the anterior cingulate cortex (Ancg) and nucleus accumbens (nAcc) regions between the schizophrenia (SZ) and control groups. (A) Glycolysis pathway in the Ancg. (B,C) Glutamate transmembrane transport and unsaturated fatty acid biosynthesis pathways in the nAcc. The horizontal axes represent groups (SZ group vs. control group), whereas the vertical axes represent GSVA enrichment scores. The filled red color indicates the SZ group and blue indicates the control group. The box plots display the median, upper and lower quartiles, and outliers of the data from each group. The scatter plots show the distribution of each data point. All *p*-values were calculated using the Wilcoxon rank-sum test.

The box plot in the GSVA revealed that the median GSVA enrichment scores of the SZ group were generally lower than those of the control group, indicating that the overall metabolic status of SZ patients may be affected by metabolic pathways such as those of glycolysis, glutamate transmembrane transport, and unsaturated fatty acid biosynthesis. SZ patients may have aberrant metabolic activity or levels of metabolites in these pathways, thus resulting in lower total GSVA enrichment scores. This may also indicate changes in cellular energy metabolism and membrane lipid metabolism in SZ patients, which might play an important part in the ferroptosis mechanism of SZ. Together, these findings suggest new avenues for further investigation into the unique mechanisms of ferroptosis in SZ.

In the present study, we systematically identified and analyzed ferroptosis-related genes and pathways in the Ancg, DLPFC, and nAcc regions of SZ patients for the first time. We also explored the associations between ferroptosis-related DEGs and age at death, postmortem interval, or brain pH. However, our study has some limitations, including a lack of experimental validation. Future studies should increase the sample size and incorporate functional trials to corroborate these findings, with the goal of investigating the precise mechanisms of ferroptosis in SZ and assessing its potential as a therapeutic target.

Conclusions

In the present study, we used multi-level gene expression and network analysis to investigate the potential relevance of ferroptosis in the pathogenesis of SZ. We observed significant changes in ferroptosis-related genes and pathways in the Ancg of SZ patients, and ferroptosis-related DEGs were negatively correlated with postmortem interval, highlighting the importance of this process in SZ. *TIMP1* and *LGALS3* were identified as key genes in the Ancg, thus warranting further investigation into their roles in disease pathophysiology and diagnostics. In the nAcc, although only one ferroptosis-related DEG was identified, the glutamate transmembrane transport pathway and unsaturated fatty acid biosynthesis process pathway showed significant differences between controls and SZ patients. These findings underscore the complex involvement of ferroptosis in SZ and suggest specific genes and pathways for future research.

Availability of Data and Materials

The datasets used or analyzed during the current study are available from the corresponding author upon reasonable request.

Yihua Jiang, *et al.*

Identification and Correlation Analysis of Ferroptosis-Related Genes in Three Brain Regions of Patients with Schizophrenia

Author Contributions

SQD, YHJ and YX designed the research study. FW and TTY performed data collection and/or processing. YX and TTY provided help and advice on the GSVA experiments. SQD analyzed the data. All authors contributed to the drafting or important editorial changes in the manuscript. All authors read and approved the final manuscript. All authors have participated sufficiently in the work and agreed to be accountable for all aspects of the work.

Ethics Approval and Consent to Participate

Not applicable.

Acknowledgment

Not applicable.

Funding

Conflict of Interest

The authors declare no conflict of interest.

References

[1] Rantala MJ, Luoto S, Borráz-León JI, Krams I. Schizophrenia: The new etiological synthesis. Neuroscience and Biobehavioral Reviews. 2022; 142: 104894.

[2] Lian K, Li Y, Yang W, Ye J, Liu H, Wang T, *et al*. Hub genes, a diagnostic model, and immune infiltration based on ferroptosis-linked genes in schizophrenia. IBRO Neuroscience Reports. 2024; 16: 317–328.

[3] Wu Q, Ren Q, Meng J, Gao WJ, Chang YZ. Brain Iron Homeostasis and Mental Disorders. Antioxidants (Basel, Switzerland). 2023; 12: 1997.

[4] Kano SI, Hodgkinson CA, Jones-Brando L, Eastwood S, Ishizuka K, Niwa M, *et al*. Host-parasite interaction associated with major mental illness. Molecular Psychiatry. 2020; 25: 194–205.

[5] Jaffe AE, Straub RE, Shin JH, Tao R, Gao Y, Collado-Torres L, *et al*. Developmental and genetic regulation of the human cortex transcriptome illuminate schizophrenia pathogenesis. Nature Neuroscience. 2018; 21: 1117–1125.

[6] Bansal V, Mitjans M, Burik CAP, Linnér RK, Okbay A, Rietveld CA, *et al*. Genome-wide association study results for educational attainment aid in identifying genetic heterogeneity of schizophrenia. Nature Communications. 2018; 9: 3078.

[7] Madrid-Gambin F, Föcking M, Sabherwal S, Heurich M, English JA, O'Gorman A, *et al*. Integrated Lipidomics and Proteomics Point to Early Blood-Based Changes in Childhood Preceding Later Development of Psychotic Experiences: Evidence from the Avon Longitudinal Study of Parents and Children. Biological Psychiatry. 2019; 86: 25–34.

[8] Maxwell AM, Rao RB. Perinatal iron deficiency as an early risk factor for schizophrenia. Nutritional Neuroscience. 2022; 25: 2218–2227.

[9] Saghazadeh A, Mahmoudi M, Shahrokhi S, Mojarrad M, Dastmardi M, Mirbeyk M, *et al*. Trace elements in schizophrenia: a systematic review and meta-analysis of 39 studies (N = 5151 participants). Nutrition Reviews. 2020; 78: 278–303.

[10] Sonnenschein SF, Parr AC, Larsen B, Calabro FJ, Foran W, Eack SM, *et al*. Subcortical brain iron deposition in individuals with schizophrenia. Journal of Psychiatric Research. 2022; 151: 272–278.

[11] Ravanfar P, Syeda WT, Jayaram M, Rushmore RJ, Moffat B, Lin AP, *et al*. In Vivo 7-Tesla MRI Investigation of Brain Iron and Its Metabolic Correlates in Chronic Schizophrenia. Schizophrenia (Heidelberg, Germany). 2022; 8: 86.

[12] Kim SW, Stewart R, Park WY, Jhon M, Lee JY, Kim SY, *et al*. Latent Iron Deficiency as a Marker of Negative Symptoms in Patients with First-Episode Schizophrenia Spectrum Disorder. Nutrients. 2018; 10: 1707.

[13] Jiang X, Stockwell BR, Conrad M. Ferroptosis: mechanisms, biology and role in disease. Nature Reviews. Molecular Cell Biology. 2021; 22: 266–282.

[14] Weiland A, Wang Y, Wu W, Lan X, Han X, Li Q, *et al*. Ferroptosis and Its Role in Diverse Brain Diseases. Molecular Neurobiology. 2019; 56: 4880–4893.

[15] Feng S, Chen J, Qu C, Yang L, Wu X, Wang S, *et al*. Identification of Ferroptosis-Related Genes in Schizophrenia Based on Bioinformatic Analysis. Genes. 2022; 13: 2168.

[16] Ramaker RC, Bowling KM, Lasseigne BN, Hagenauer MH, Hardigan AA, Davis NS, *et al*. Post-mortem molecular profiling of three psychiatric disorders. Genome Medicine. 2017; 9: 72.

[17] Barrett T, Wilhite SE, Ledoux P, Evangelista C, Kim IF, Tomashevsky M, *et al*. NCBI GEO: archive for functional genomics data sets–update. Nucleic Acids Research. 2013; 41: D991–D995.

[18] Robinson MD, McCarthy DJ, Smyth GK. edgeR: a Bioconductor package for differential expression analysis of digital gene expression data. Bioinformatics (Oxford, England). 2010; 26: 139–140.

[19] Yang F, Xiao Y, Ding JH, Jin X, Ma D, Li DQ, *et al*. Ferroptosis heterogeneity in triple-negative breast cancer reveals an innovative immunotherapy combination strategy. Cell Metabolism. 2023; 35: 84–100.e8.

[20] Szklarczyk D, Morris JH, Cook H, Kuhn M, Wyder S, Simonovic M, *et al*. The STRING database in 2017: quality-controlled protein-protein association networks, made broadly accessible. Nucleic Acids Research. 2017; 45: D362–D368.

[21] Saito R, Smoot ME, Ono K, Ruscheinski J, Wang PL, Lotia S, *et al*. A travel guide to Cytoscape plugins. Nature Methods. 2012; 9:

1069–1076.

[22] Chin CH, Chen SH, Wu HH, Ho CW, Ko MT, Lin CY. cytoHubba: identifying hub objects and sub-networks from complex interactome. BMC Systems Biology. 2014; 8: S11.

[23] Robin X, Turck N, Hainard A, Tiberti N, Lisacek F, Sanchez JC, *et al*. pROC: an open-source package for R and S+ to analyze and compare ROC curves. BMC Bioinformatics. 2011; 12: 77.

[24] Linden A. Measuring diagnostic and predictive accuracy in disease management: an introduction to receiver operating characteristic (ROC) analysis. Journal of Evaluation in Clinical Practice. 2006; 12: 132–139.

[25] Zou KH, O'Malley AJ, Mauri L. Receiver-operating characteristic analysis for evaluating diagnostic tests and predictive models. Circulation. 2007; 115: 654–657.

[26] Hänzelmann S, Castelo R, Guinney J. GSVA: gene set variation analysis for microarray and RNA-seq data. BMC Bioinformatics. 2013; 14: 7.

[27] Brunson JC. ggalluvial: Layered Grammar for Alluvial Plots. Journal of Open Source Software. 2020; 5: 2017.

[28] Yan HF, Zou T, Tuo QZ, Xu S, Li H, Belaidi AA, *et al*. Ferroptosis: mechanisms and links with diseases. Signal Transduction and Targeted Therapy. 2021; 6: 49.

[29] Masaldan S, Bush AI, Devos D, Rolland AS, Moreau C. Striking while the iron is hot: Iron metabolism and ferroptosis in neurodegeneration. Free Radical Biology & Medicine. 2019; 133: 221–233.

[30] Stockwell BR, Friedmann Angeli JP, Bayir H, Bush AI, Conrad M, Dixon SJ, *et al*. Ferroptosis: A Regulated Cell Death Nexus Linking Metabolism, Redox Biology, and Disease. Cell. 2017; 171: 273–285.

[31] Dixon SJ, Lemberg KM, Lamprecht MR, Skouta R, Zaitsev EM, Gleason CE, *et al*. Ferroptosis: an iron-dependent form of nonapoptotic cell death. Cell. 2012; 149: 1060–1072.

[32] Rao J, Qian X, Li G, Pan X, Zhang C, Zhang F, *et al*. ATF3-mediated NRF2/HO-1 signaling regulates TLR4 innate immune responses in mouse liver ischemia/reperfusion injury. American Journal of Transplantation: Official Journal of the American Society of Transplantation and the American Society of Transplant Surgeons. 2015; 15: 76–87.

[33] Hartman MG, Lu D, Kim ML, Kociba GJ, Shukri T, Buteau J, *et al*. Role for activating transcription factor 3 in stress-induced beta-cell apoptosis. Molecular and Cellular Biology. 2004; 24: 5721–5732.

[34] Hunt D, Hossain-Ibrahim K, Mason MRJ, Coffin RS, Lieberman AR, Winterbottom J, *et al*. ATF3 upregulation in glia during Wallerian degeneration: differential expression in peripheral nerves and CNS white matter. BMC Neuroscience. 2004; 5: 9.

[35] Cabral-Pacheco GA, Garza-Veloz I, Castruita-De la Rosa C, Ramirez-Acuña JM, Perez-Romero BA, Guerrero-Rodriguez JF, *et al*. The Roles of Matrix Metalloproteinases and Their Inhibitors in Human Diseases. International Journal of Molecular Sciences. 2020; 21: 9739.

[36] Agnello L, d'Argenio A, Caliendo A, Nilo R, Zannetti A, Fedele M, *et al*. Tissue Inhibitor of Metalloproteinases-1 Overexpression Mediates Chemoresistance in Triple-Negative Breast Cancer Cells. Cells. 2023; 12: 1809.

[37] Li HY, Yang S, Li JC, Feng JX. Galectin 3 inhibition attenuates renal injury progression in cisplatin-induced nephrotoxicity. Bioscience Reports. 2018; 38: BSR20181803.